Prepublished copy

Nature Environment & Pollution Technology

This is a peer-reviewed prepublished version of the paper to be published in Vol. 25, No. 1, March 2026 issue

Original Research

Air Aware IoT: Low-Cost Sensor Solutions for Urban Pollution Monitoring and Public Health

K. Venugopala Rao[1], Ch. Mani Kumar[1]†, V. Saritha[2] and B. Kanthamma[3]

[1]Department of Physics, GITAM Deemed to be University, Visakhapatnam-530045, Andhra Pradesh, India

[2]Department of Environmental Science, GITAM Deemed to be University, Visakhapatnam-530045, Andhra Pradesh, India

[3]Department of Electrical, Electronics and Communication Engineering, GITAM Deemed to be University, Visakhapatnam-530045, Andhra Pradesh, India

†Corresponding author: Ch. Mani Kumar; mchimpin@gitam.edu

ORCID IDs of Authors

K. Venugopala Rao: https://orcid.org/0009-0001-5451-2066

Ch. Mani Kumar: https://orcid.org/0000-0003-4035-4076

V. Saritha: https://orcid.org/0000-0003-0473-993X

Key Words	Air pollution, $PM_{2.5}$, O_3, CO_2, TVOC, Raspberry Pi, IoT
DOI	https://doi.org/10.46488/NEPT.2026.v25i01.B4328 (DOI will be active only after the final publication of the paper)
Citation for the Paper	Rao, K.V., Mani Kumar, C., Saritha, V. and Kanthamma, B., 2026. Air aware IoT: low-cost sensor solutions for urban pollution monitoring and public health. *Nature Environment and Pollution Technology*, 25(1), p. B4328. https://doi.org/10.46488/NEPT.2026.v25i01.B4328

ABSTRACT

Air pollution, especially in cities, has a considerable impact on human health, contributing to global morbidity and mortality rates. With urban populations increasing and public awareness of air quality being low, there is an urgent need for low-cost, portable devices to monitor airborne contaminants in indoor and outdoor settings. This work shows the design and functionality of a low-cost, portable device capable of measuring major air quality parameters, such as gaseous pollutants (CO_2, O_3, TVOC, and $PM_{2.5}$) and physical indicators (temperature and humidity). The device connects various sensors to an ATmega microcontroller via a signal conditioning circuit, solving current, format, and speed incompatibilities. Data processed by the microcontroller is sent to various devices using IoT technology. The device accurately measures ozone, $PM_{2.5}$, temperature, and humidity with precisions of ±5.02 µg/m³, ±7.94 µg/m³, ±0.67°C, and ±1.68%, respectively. The results demonstrate the system's dependability in air quality monitoring, providing an affordable and accessible alternative for environmental surveillance. This innovation has the potential to raise public awareness and enable large-scale pollution monitoring activities, making it a useful tool for minimizing the negative consequences of air pollution on public health.

INTRODUCTION

Air pollution poses a significant threat to global public health, exacerbated by rapid urbanization and industrial growth (Kortoçi et al. 2022). Urban areas, characterized by dense populations, transportation networks, and industrial activity, are particularly vulnerable to elevated pollutant levels. Globally, air pollution contributes to over 7 million premature deaths annually due to respiratory diseases, cardiovascular disorders, and lung cancer, with 90% of the world's population exposed to pollutant concentrations exceeding World Health Organization (WHO) guidelines (Jiang et al. 2016, Meo et al. 2021). These alarming statistics underscore the need for robust air quality monitoring systems to inform policy reforms and mitigate health risks (Perillo et al. 2022).

Existing regulatory monitoring networks, though critical, are often limited in spatial coverage and cost, restricting their deployment to specific urban zones (Baca-López et al. 2021). To address this gap, recent studies emphasize integrating low-cost sensors with traditional networks to enhance spatial resolution and data accessibility, particularly in underserved areas (Motlagh et al. 2021, Shindler 2021). However, conventional monitoring systems face challenges such as high power consumption, complex circuitry, and frequent calibration requirements, limiting their practicality for widespread deployment (Castell et al. 2013, Idrees et al. 2018).

Among pollutants, particulate matter ($PM_{2.5}$) and ground-level ozone (O_3) are particularly hazardous due to their ability to penetrate deep into the respiratory system and exacerbate conditions such as asthma and cardiovascular disease (Meo et al. 2021). $PM_{2.5}$ exposure is linked to elevated mortality rates, especially among vulnerable populations such as pregnant women and the elderly, while tropospheric ozone formed through reactions between vehicle emissions and sunlight poses severe risks in both indoor and outdoor environments (Cao & Thompson 2016). These health impacts necessitate affordable, portable devices capable of real-time, multi-parameter monitoring to complement existing infrastructure.

Recent advancements in IoT-enabled devices show great potential for enhancing air quality monitoring. However, many systems remain confined by low sensor precision, a single-parameter concentration, and reliance on bulky or resource-bound hardware. For instance, wireless networks using ATmega328P microcontrollers have been deployed for indoor air quality monitoring, but face memory constraints (Abraham & Li 2014), while mobile applications for outdoor pollution tracking often lack precision (Kodali & Sarjerao 2018). More recent advances, such as the IoT-based APM box, which incorporates machine learning to improve the calibration of low-cost sensors like MQ-7 and MQ-131, provide greater pollutant measurement reliability (Rathnayake et al. 2024). Bi-LSTM (Bidirectional Long Short-Term Memory) models optimized with metaheuristic algorithms like the Osprey Optimization Algorithm (OOA) have shown promising results for accurate $PM_{2.5}$ concentration estimation when paired with meteorological data (Saminathan and Malathy 2024).

However, extensive calibration and environmental validation are still required to ensure the wider applicability of these technologies.

This study aims to design and validate a low-cost, portable, multi-sensor IoT device for real-time air quality monitoring in urban areas. To achieve this, a compact system was developed using a Raspberry Pi and an ATmega microcontroller to measure particulate matter ($PM_{2.5}$), ozone (O_3), total volatile organic compounds (TVOC), carbon dioxide (CO_2), temperature and humidity. Although the system's primary emphasis is on effective hardware integration, it presents a practical and scalable solution by strategically combining multiple low-cost sensors into a compact, portable, and IoT-enabled device. A custom signal conditioning circuit was implemented to address sensor incompatibilities, and Python-based software with IoT connectivity enables real-time data visualization on both local and remote devices. Its novelty lies in the synergistic integration of diverse sensors for comprehensive air quality monitoring, real-time data transmission for accessible urban deployment, and its adaptability for use across varied environmental settings. This approach offers a scalable and cost-effective solution to address spatial coverage limitations in urban air quality monitoring, making it particularly suited for city-wide deployment and community-based environmental tracking.

2. MATERIALS AND METHODS

2.1 Instrumentation

The system's hardware architecture includes a processing unit with a Raspberry Pi, an ATmega microcontroller, and other critical components, as shown in Fig. 1. The sensors used in the sensing unit are described in Table 1. Furthermore, Fig. 2. depicts the physical implementation of the portable device, emphasizing its compact and modular architecture. Fig. 3. depicts the data transmission process from the device to IoT-enabled platforms, highlighting its seamless connectivity and real-time monitoring capabilities.

To allow portability and outdoor use, the system is powered by a 5V USB supply, typically via a rechargeable power bank or wall adapter. It consumes approximately 350–400 mA during continuous operation, enabling several hours of uninterrupted monitoring. As shown in Fig. 2, all internal components are housed within a compact plastic enclosure. While not industrially ruggedized, the casing provides basic protection against dust, light moisture, and handling, making it suitable for short-term urban and semi-outdoor deployments.

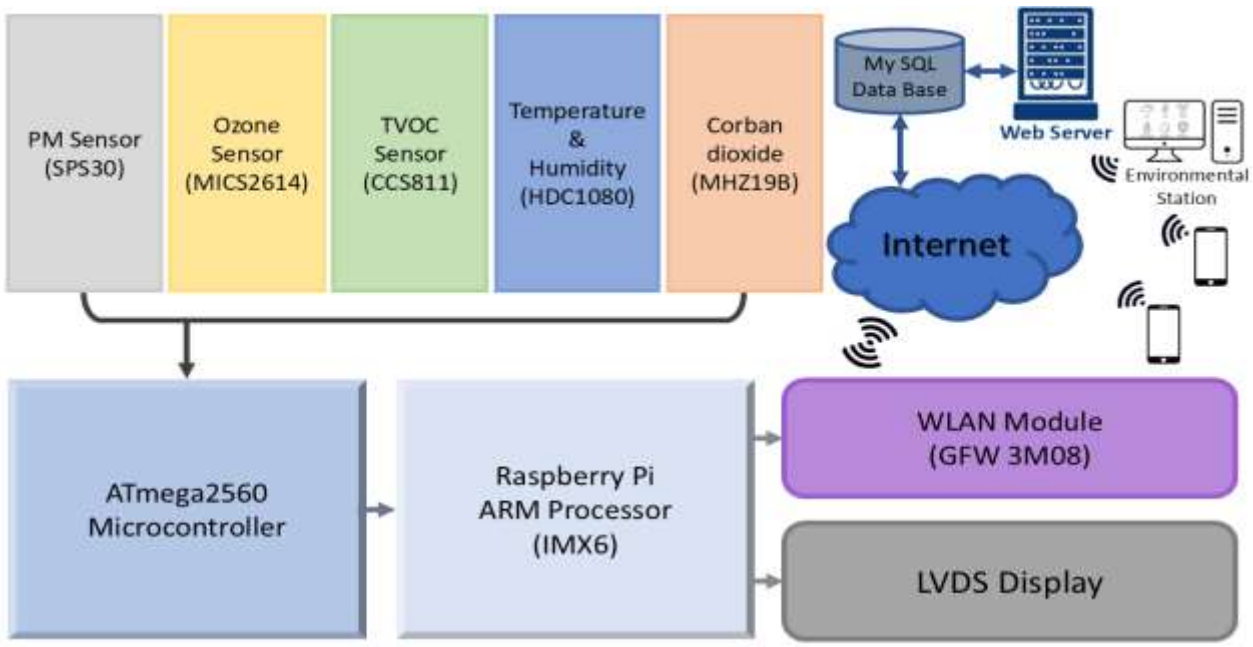

Fig. 1: Block diagram of a Portable device for measuring indoor and outdoor Air pollutants

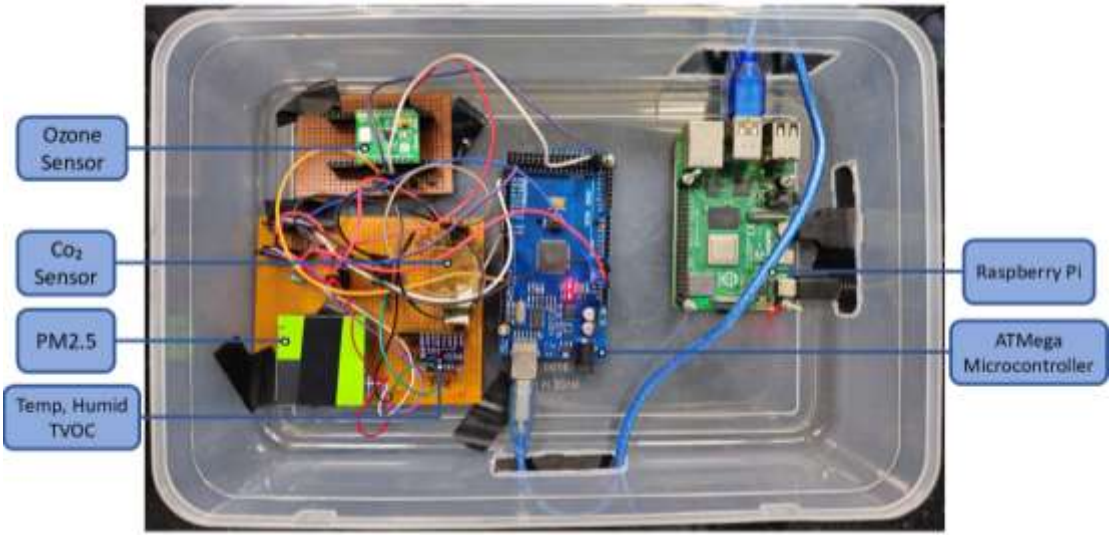

Fig. 2: Hardware Setup for a Portable Environmental Monitoring System

Table 1: Sensors used in the sensing unit

Sensor Name	Measured Parameter	Range	Accuracy
SPS30	Particulate Matter	0 to 1000 µg/m³	±10 µg/m³
MiCS2614	Ozone	10 to 1000 ppb	--
CCS811	TVOC	0 to 1187 ppb	±15%
MHZ19B	CO_2	0 to 5000 ppm	±50 ppm + 3% of reading
HDC1080	Temperature & Humidity	-40°C to 125°C, 0% to 100%	±0.2°C, ±2%

The system's sensing unit incorporates various sensors, including the MICS 2614 ozone sensor, the SPS30 particulate matter sensor, the CCS811 TVOC sensor, the MHZ19B CO_2 sensor and the HDC1080 temperature

and humidity sensor. The system processing layer is composed of an ATmega microcontroller (Al-Kofahi et al. 2019) and a Raspberry Pi (Vivek et al. 2017). Utilizing the protocols, the ATmega microcontroller reads the sensor data through the signal conditioning circuit and processes the information.

The Raspberry Pi can run a software stack, comprised of an operating system, a web server, a database, and a programming language. It has an execution speed of up to 1.2 GHz and can run operating systems like Android and Linux. The communication layer of the system contains a WLAN module linked with the processor to transmit sensor data to various IoT-enabled devices. The data analyzing layer of the system displays the environmental parameters on an LVDS (Low Voltage Differential Signalling) monitor and stores them in the database.

Most sensors used in the system provide factory-calibrated digital outputs, eliminating the need for manual calibration. The system uses temperature compensation and CRC-based checksum verification to achieve real-time software-level validation to guarantee data integrity, as shown in the software flow diagram (Fig. 4). The prototype's performance was evaluated by placing it at a site where an APPCB (Andhra Pradesh Pollution Control Board) monitoring station was already in place. The APPCB reference values for that location were compared with the data that the gadget collected over a 24-hour period. The accuracy of the system was robustly validated at the field level through the use of statistical metrics such as Mean Absolute Error (MAE), Root Mean Square Error (RMSE), and Mean Bias (MB) to assess the results.

Fig. 3: Mechanism of Data Transmission to IoT Platforms

2.2 Interfacing of Particulate Matter Sensor

The SPS30 optical sensor is crucial for the precise measurement of 2.5-micrometre-diameter particles ($PM_{2.5}$), leveraging laser scattering technology. Renowned for its stability and contamination resistance, the

sensor features a built-in fan for controlled airflow, regulated through an internal feedback loop. Airborne particles passing through a laser beam generate light scattering, processed by algorithms on the SPS30's microcontroller, yielding accurate mass concentration output. This comprehensive integration ensures robust performance across diverse environmental conditions.

2.3 Interfacing of Ozone Sensor

To monitor ozone concentrations, the MICS-2614, a MOS-type sensor, is employed with a measuring range of 10 to 1000 ppb. The sensor module integrates heating circuits along its edges and a sensing material. The heating circuit, powered by a voltage source, warms the sensing material by connecting the heater to the supply voltage through a resistor, forming a voltage divider circuit. The MCP 3201 (ADC) operates within a voltage range of 2.7V to 5.5V and employs a successive approximation register (SAR) architecture. Communication between the microcontroller and ADC is facilitated through the SPI protocol. Eq. (1) is to derive ozone concentration from the measured ADC data.

$$\text{Ozone concentration [in ppb]} = 10^{\left(\frac{2566-(\text{ADC value}-584)}{1283}\right)} + 1 \quad \ldots (1)$$

2.4 Interfacing of TVOC Sensor

The CCS811 sensor, designed for TVOC concentration measurement, integrates a microcontroller and an analog-to-digital converter. The analog output from internal ADC converts into a digital signal and is processed by the microcontroller. Interfacing with the host microcontroller is established through the SDA and SCL pins and operating within a current range of up to 30mA and a voltage range of 1.8 to 3.6 volts, the sensor maintains energy efficiency, consuming only 46mW.

2.5 Interfacing of Carbon Dioxide Sensor

The MHZ19B, a non-dispersive infrared (NDIR) sensor, is employed to monitor ambient CO_2 concentration. It consists of an infrared source, optical filter, detector, and gas chamber. The emitted infrared light, closely matching the absorption band of CO_2, facilitates the accurate identification of CO_2 molecules. As light traverses the gas chamber, CO_2 molecules absorb specific wavelengths, and the detector measures the unabsorbed light, converting it into voltage. CO_2 concentration is gauged by analyzing the on and off times of the PWM output, connected to a PWM-compatible GPIO pin on the microcontroller. Additionally, the sensor is configured in UART mode, connecting to the transmitter and receiver pins of the controller. The on-time and off-time of the signal, extracted from the PWM output, are then substituted into Eq. (2) to derive the carbon dioxide concentration in parts per million (ppm). This integration of PWM and UART modes enhances the precision of CO_2 measurement.

$$CO_2 \text{ [in ppm]} = \frac{Maximum\ detection\ range \times (T_{ON} - Cycle\ Start\ high\text{-}level\ output)}{T_{ON} + T_{OFF} - Cycle\ Start\ high\text{-}level\ output - Cycle\ End\ level\ output} \quad \ldots (2)$$

2.6 Interfacing of Temperature and Humidity Sensor

The HDC1080 sensor, connected to the microcontroller through the I2C protocol for atmospheric temperature and relative humidity measurement, operates as a digital moisture and temperature sensor. Notably, this factory-calibrated sensor eliminates the need for user calibration. The sensor boasts high precision, with a ±2% accuracy for relative humidity and ±0.2°C for temperature.

2.7 Software Implementation

The software is responsible for controlling different hardware devices in the system. The basic concept inside embedded software is to control the operation of a group of hardware components without sacrificing their purpose or efficiency. The Raspberry Pi supports various software utilities like an operating system, a web server, a database, and a scripting language for web development. In the present system, a Linux operating system is used, the Apache HTTP server is used to develop a web server, MySQL is used for database management, and a PHP scripting language is used for web servers. The software implementation in this study is divided into two sections: the first is the Embedded C programming language, which is used to connect the sensors to an ATmega microcontroller. In the second section, the software stack, which runs on the Raspberry Pi, stores and distributes data among IoT-enabled devices. Fig. 4 depicts the software implementation flowchart. The graphical user interface is built by creating PHP-scripted web pages that display the current environmental data and previous data stored in the database.

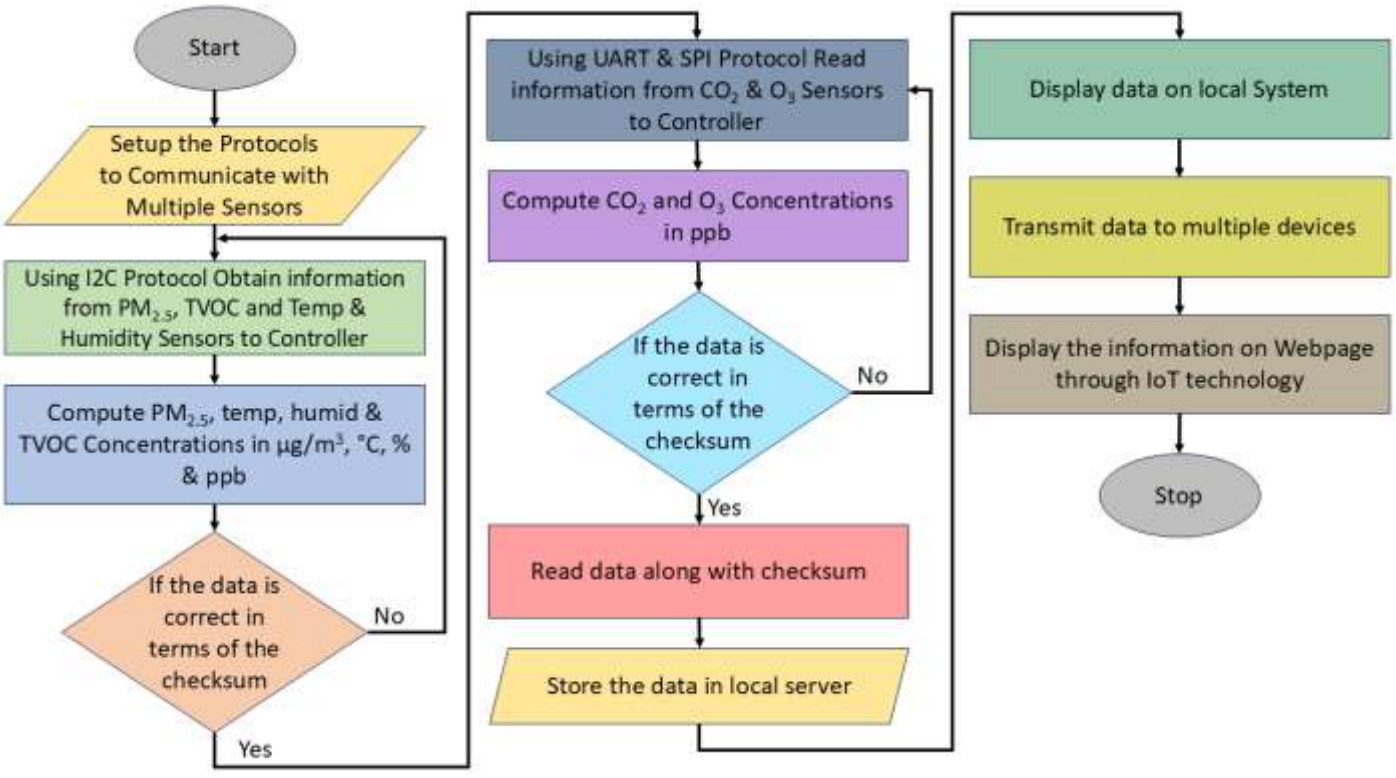

Fig. 4: Software flow diagram showing sensor communication protocols, temperature compensation, checksum validation, and IoT-based data transmission

3. RESULTS AND DISCUSSIONS

3.1 Monitoring Locations and System Deployment

The system was engineered to assess air pollutant concentrations across seasons, exploring variations in environmental conditions. Measurements in four locations in Visakhapatnam were compared with Andhra Pradesh Pollution Control Board (APPCB) standards. Continuous 24-hour measurements illuminated pollutant fluctuations in GVMC (Greater Visakhapatnam Municipal Corporation) (high population), PORT (industrial), NAD (Naval Armament Depot) (traffic), and GITAM (Gandhi Institute of Technology and Management) (green – Control Zone / Vegetative Zone). Fig. 5. illustrates the placement of the monitoring device at GVMC and NAD locations. The system effectively gauges O_3, $PM_{2.5}$, CO_2, TVOC, temperature, and humidity. The system allows for a quick response to any spikes in pollution levels. By monitoring these key pollutants and environmental conditions, the system provides valuable data for decision-makers to implement targeted interventions to improve air quality in Visakhapatnam. This proactive approach can help mitigate the health risks associated with poor air quality and contribute to a healthier environment for city residents. Furthermore, the data collected can also be used to track trends over time and assess the effectiveness of implemented interventions. This extensive monitoring system is essential for establishing a sustainable and healthier future for Visakhapatnam.

Fig. 5: The system was placed at NAD and GVMC locations in Visakhapatnam

3.2 Sampling and Data Collection

The prototype was deployed for 24 hours at each of the four monitoring sites – GVMC, PORT, NAD, and GITAM during each of the four seasons: summer, monsoon, autumn, and winter. This resulted in a total of 96 monitoring hours per location. Environmental data was recorded at 30-second intervals, yielding approximately 11,520 readings per sensor per site (96 hours × 60 minutes × 2 readings per minute). Data integrity was ensured through checksum validation during acquisition. No additional filtering or smoothing techniques were applied.

The validated data was then aggregated into hourly averages to align with standard reporting intervals, enabling seasonal trend analysis and comparison with APPCB reference data. A summary of the seasonal deployment, sampling strategy, and pre-processing steps is provided in Table 2.

Table 2: Summary of Sampling and Pre-processing

Location	Seasons Covered	Monitoring Duration	Sampling Frequency	Total Readings (per sensor)	Data Aggregation	Pre-processing Techniques
GVMC PORT NAD GITAM	Summer, Monsoon, Autumn, Winter	384 hours (24 h x 4 Seasons x 4 Locations)	Every 30 seconds	11,520	Hourly averages	Checksum validation only

3.3 Quantitative Error Analysis

The accuracy of the developed system was evaluated across various monitoring sites using statistical metrics, including Mean Absolute Error (MAE), Root Mean Square Error (RMSE), and Mean Bias (MB). As shown in Table 3, the average values for O_3, $PM_{2.5}$, Temperature, and Humidity remained within acceptable limits, confirming the system's capability for consistent air quality monitoring. MAE values across pollutants were uniformly low, with minimal RMSE and bias, reflecting robust and precise sensor performance. Locations such as GVMC and NAD exhibited balanced metrics across all parameters, whereas PORT recorded higher $PM_{2.5}$ error, suggesting localized variability. Despite these differences, the system consistently produced accurate and reproducible measurements at all sites, demonstrating its suitability as a low-cost, scalable solution for urban environmental monitoring.

Table 3: Average MAE, RMSE, and MB values for O_3, $PM_{2.5}$, Temperature, and Humidity across all monitoring locations.

Location	MAE				RMSE				MB			
	O_3	$PM_{2.5}$	Temp.	Humidity	O_3	$PM_{2.5}$	Temp.	Humidity	O_3	$PM_{2.5}$	Temp.	Humidity
GVMC	0.719	2.480	0.540	0.342	0.636	3.667	0.595	0.055	-0.636	-3.667	-0.190	0.050
PORT	1.091	3.500	0.312	0.772	0.273	6.500	0.370	0.487	0.092	-6.500	0.145	-0.487
NAD	0.758	1.973	0.367	0.312	0.607	1.857	0.530	0.387	-0.607	-0.357	-0.380	-0.387
GITAM	1.134	2.417	0.382	1.080	0.878	1.885	0.448	0.715	0.633	-1.115	-0.412	0.440

3.4 Correlation Analysis and Observations

3.4.1 Ozone Dynamics: A Spatial and Temporal Analysis

Throughout this study, the prototype was strategically positioned in four distinct locations, each corresponding to a unique season. Continuous measurements were meticulously conducted for a comprehensive

24-hour period. The collected data was then meticulously compared against the benchmarks established by the Andhra Pradesh Pollution Control Board (APPCB), India.

Higher O_3 levels were recorded at the three sampling sites—GVMC, PORT, and NAD. Though the values were noted to be higher in comparison to other seasons, these were within the limits, as the sampling was done during the COVID-19 pandemic, when human and industrial activities were restricted. Higher concentrations of ozone can be attributed to localized pollutant emissions (Mohtar et al. 2018), while lower concentrations at GITAM are attributed to the dispersion of pollutants due to sea breezes (Latif et al. 2012). Even though O_3 is not a primary pollutant, its formation is triggered by oxides of nitrogen and hydrocarbons by reacting with sunlight. Owing to the tropical zone and the availability of O_3 concentrations were recorded to be as high as 60 $\mu g/m^3$. Nitrogen dioxide is an essential factor that influences the daily variations of O_3. The higher concentrations of O_3 during late afternoon hours are attributed to the long daylight hours (Lv et al. 2022).

Fig. 6. presents Pearson's correlation analysis, highlighting linear positive relationships ranging from moderate to very high between measured and standard ozone levels across four locations and seasons. The heat map visually depicts correlation coefficients, showcasing the degree of correlation between concentrations recorded by the developed system and APPCB standards. The colour intensity reflects the strength of these correlations, with values close to 1 indicating a strong positive relationship. This graph offers a concise overview of ozone measurements' seasonal consistency and reliability at each location.

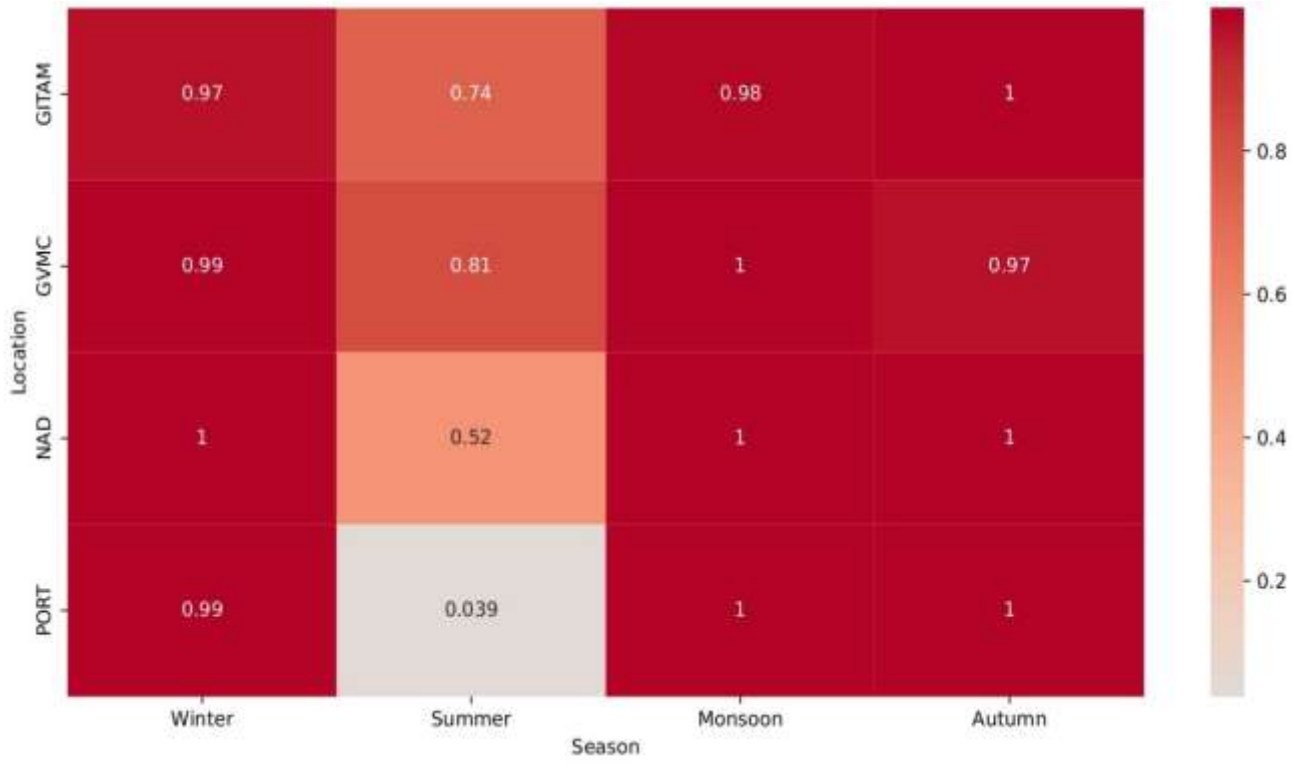

Fig. 6: Pearson Correlation of Seasonal Ozone Levels in Four Urban Locations

The analysis reveals a consistently high correlation across most seasons and locations, indicating strong alignment between measured and standard O_3 levels. During the winter season, correlations at all test locations are exceptionally high, ranging from 0.97 to 1. This suggests that O_3 levels are almost perfectly aligned with standards, reflecting reliable monitoring and stable environmental conditions. GVMC and NAD have reasonable correlations of 0.81 and 0.52, respectively, but the PORT location has a significantly low correlation of only 0.039. This fast fall is most likely due to measurement errors. The monsoon season returns to significant correlations across all locations, with values approaching or equal to one, showing that measurements capture O_3 levels well during this period. This suggests that the accuracy of measurements improves during the monsoon season, possibly due to less variability in environmental factors. Overall, the data indicate that O_3 levels are more reliably captured during the monsoon season compared to other times of the year.

3.4.2 $PM_{2.5}$ Dynamics: A Spatial and Temporal Analysis

The peak emission of particulate matter was noted between 6 AM to 12 PM and 12 PM to 6 PM near GVMC during the Monsoon season. This diurnal variation is due to human activities and precisely to vehicular movement by the population to work and businesses. The $PM_{2.5}$ formed due to combustion is understood to be more hazardous as it can reach the lungs and bloodstream owing to its smaller dimensions. Changes in human activities have shown a significant impact on differences in the concentration of air pollutants at various times of the day.

Fig. 7. visually represents the results of bivariate correlation analysis, illustrating the dispersion between concentrations measured by the developed system and the standard set by APPCB. The values of the Pearson correlation coefficient (r) for the GVMC area ranged from 0.98 (winter) to 0.81 (autumn), portraying a robust and positive linear relationship. The PORT area's coefficients varied from 0.92 (winter and monsoon) to 0.79 (summer and autumn), indicating a substantial correlation. NAD area exhibited correlations from 0.98 (winter) to 0.92 (monsoon), underlining a commendable association. Similarly, the GITAM area demonstrated strong correlations, ranging from 0.99 (winter) to 0.89 (summer). These correlations demonstrate the system's effectiveness in accurately capturing the variations in $PM_{2.5}$ concentrations across different seasons and locations.

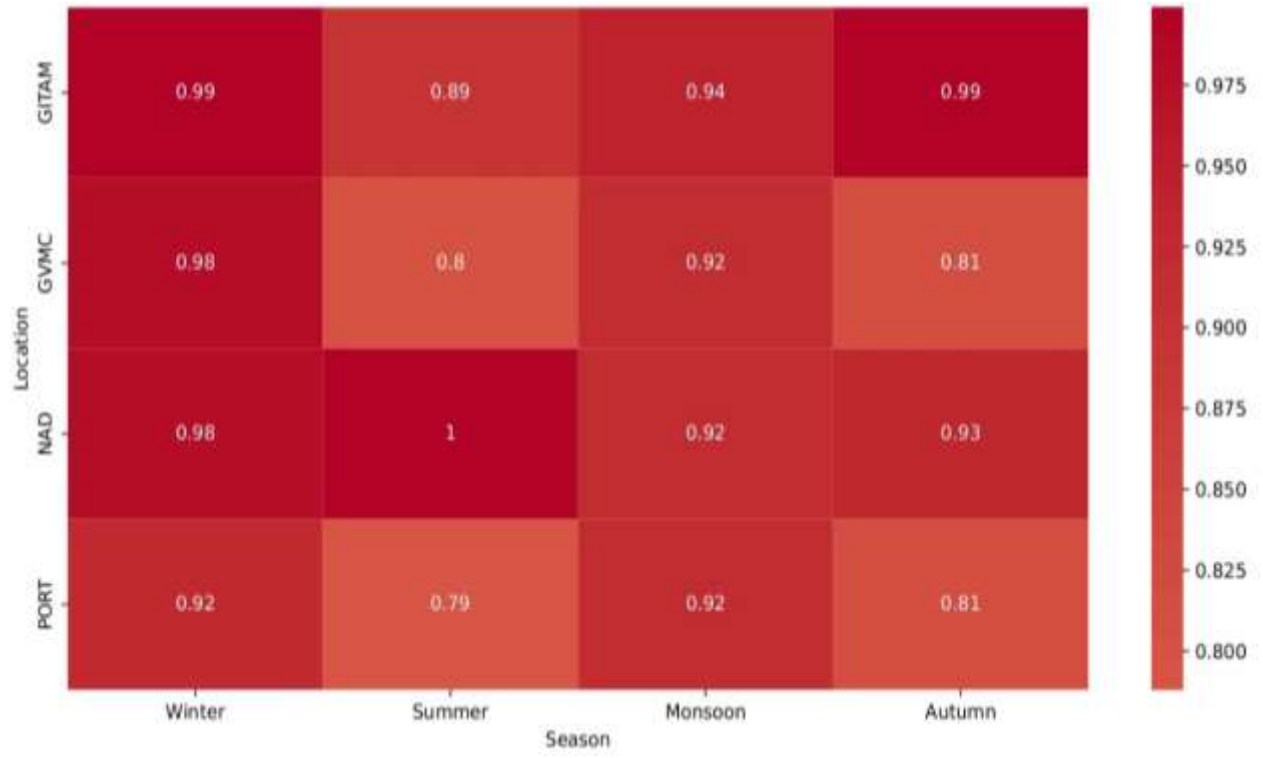

Fig. 7: Pearson Correlation of Seasonal $PM_{2.5}$ Levels in Four Urban Locations

3.4.3 Temperature and Humidity Dynamics: A Spatial and Temporal Analysis

GITAM had the lowest winter temperatures, most likely due to its green surroundings, which encourage cooling via flora. In contrast, the highest temperatures were recorded in the PORT region, which was ascribed to industrial activity that generated tremendous heat. Summer temperatures rose in GVMC, a densely populated area with significant urban heat island effects. During the monsoon, PORT and NAD had the greatest temperatures, which were impacted by PORT industrial pollutants and NAD heavy traffic. In fall, the PORT area had the greatest and lowest temperatures, reflecting industrial heat during the day and cooling influences near the seaside at night. The average temperature concentration over seasons was compared to APPCB standard values, with an accuracy of ±0.67°C.

During the winter, GVMC had elevated relative humidity due to high human density and water vapour emissions, whereas PORT had the lowest values, most likely due to industrial heat lowering moisture. In the summer, PORT had the most humidity, owing to its coastal vicinity and industrial cooling, whereas GITAM had the lowest due to its verdant surroundings and less human activity. During the monsoon, GVMC had the highest humidity, which was caused by rainfall and urban moisture retention, whereas PORT had the lowest, presumably due to industrial pollutants. In the autumn, GVMC again had the highest humidity due to urban density and adjacent water sources, whereas PORT had the lowest due to industrial heat. Across all seasons, the six-hour average humidity was compared to APPCB requirements and achieved ±1.68% accuracy.

Fig. 8 and 9 visually portray the outcomes of bivariate correlation analysis, showcasing the dispersion between concentrations measured by the developed system and the standards set by APPCB. The bivariate correlation analysis revealed strong positive relationships between the concentrations measured by the developed system and the standards set by APPCB across all locations and seasons. In the GVMC area, the coefficients were consistently high, ranging from 0.99 to 1.00, indicating a robust correlation. Similarly, in the PORT area, the coefficients ranged from 0.99 to 1.00, signifying a strong and consistent positive correlation. In the NAD area, the coefficients showed a strong positive correlation, ranging from 0.92 to 1.00. The GITAM area exhibited strong positive correlations, with coefficients ranging from 0.97 to 1.00 across different seasons. These findings emphasize the reliability and accuracy of the developed system in measuring pollutant concentrations in diverse environmental conditions.

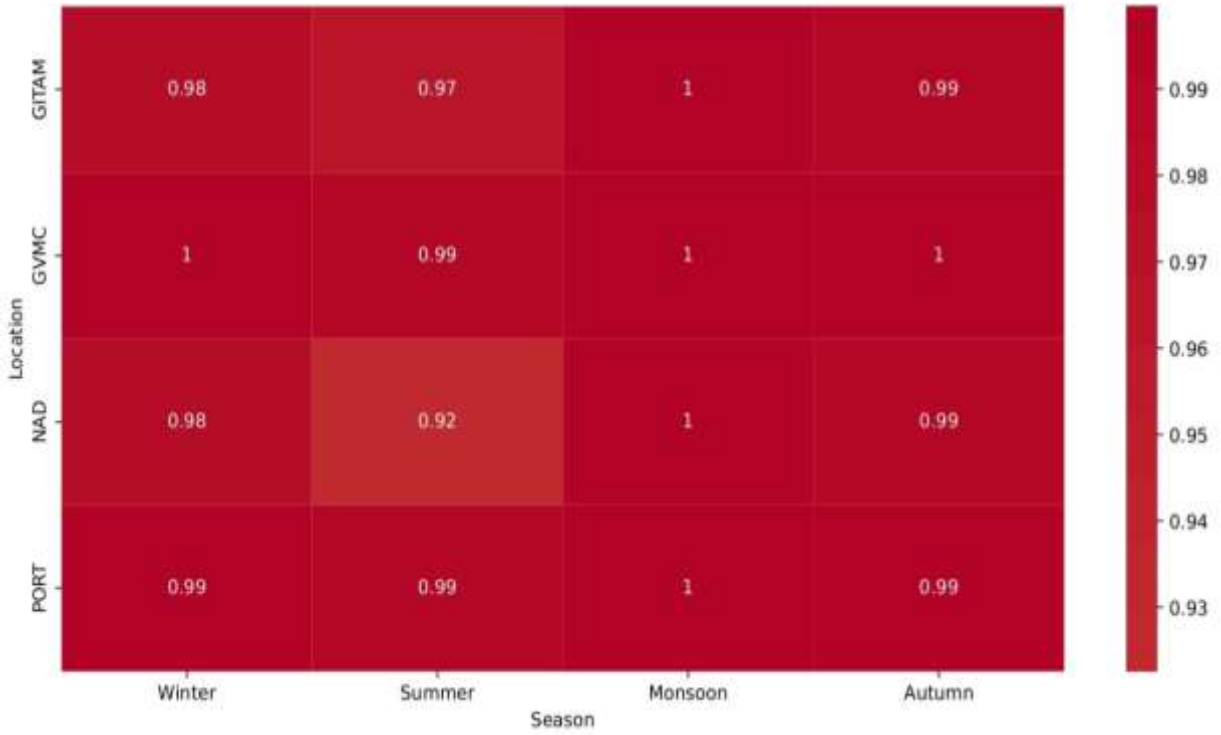

Fig. 8: Pearson Correlation of Seasonal Temperature Levels in Four Urban Locations

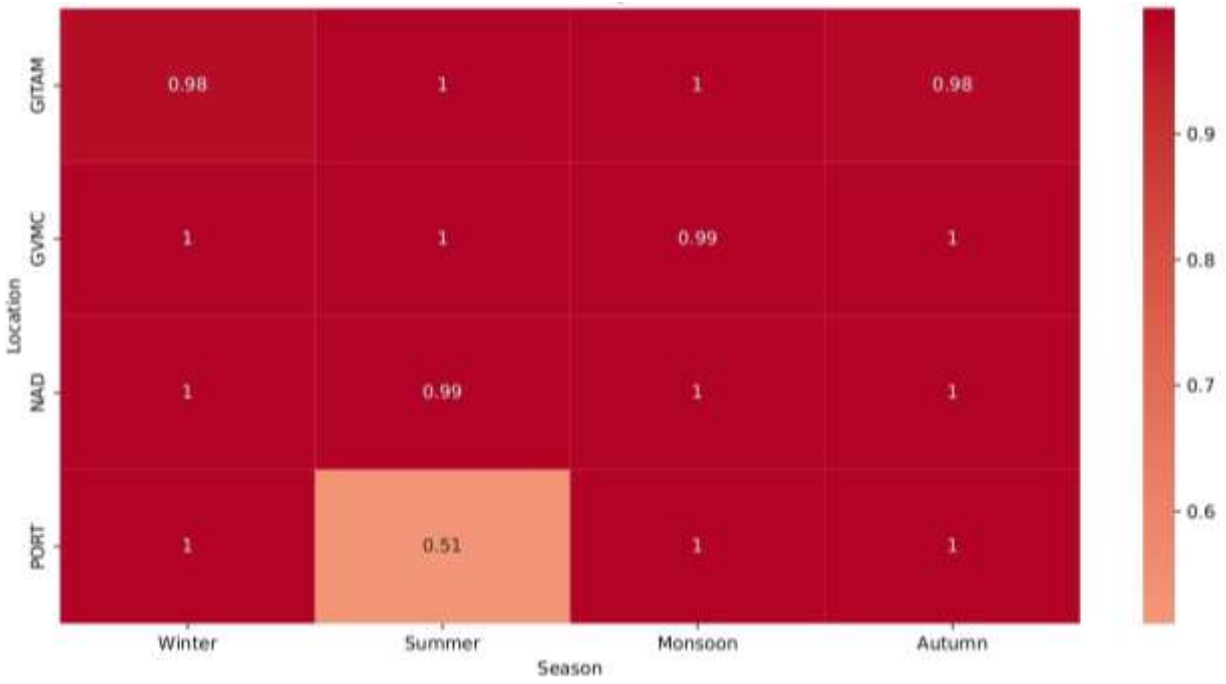

Fig. 9: Pearson Correlation of Seasonal Humidity Levels in Four Urban Locations

In the GVMC area, a consistently strong correlation was observed across all seasons, with coefficients ranging from 0.99 to 1.00, indicating a robust agreement between measured and standard values. The PORT area displayed a slightly lower correlation in the summer season (0.51), but in other seasons, it exhibited a strong correlation (1.00). Similarly, the NAD area maintained a robust correlation (1.00) across all seasons. In the GITAM area, while maintaining a generally strong correlation, a minor decrease was observed in the winter and autumn seasons (0.98). These findings emphasize the reliability of the developed system's measurements, aligning closely with the established standards.

3.5 Seasonal Variation of Pollutants

Pollutant concentrations were recorded to be higher during monsoon and autumn due to the adverse meteorological conditions that would enhance the accumulation of pollutants, which can be aggravated due to increased humidity conditions (Johnson 2022, Wang et al. 2022). Previous studies have also reported that lower temperatures and wind speed would also enhance particulate matter concentrations as the meteorological conditions tend to trap these pollutants, inhibiting their transportation outward. Further, higher humidity and low temperature also favour the conversion of semi-volatile species to aerosol phase leading to higher concentrations of particulate matter. Our study was in line with the reports confirming higher concentrations of pollutants during monsoon and winter, along with O_3 since the city's average temperatures during these seasons were the same as in other seasons.

4. CONCLUSION AND FUTURE WORKS

The current work presents the development of a compact air quality monitoring system built on a single-board computer and an ATmega microcontroller. The system integrates intelligent sensors to monitor O_3, $PM_{2.5}$, CO_2, TVOC, temperature, and relative humidity in both indoor and outdoor environments. Designed to be portable and cost-effective, the device operates with a 30-second sampling interval, enabling high-frequency data collection. Its IoT-enabled architecture supports real-time data transmission and remote access, making it suitable for individual use as well as community-scale monitoring. The low overall cost of the device enhances its scalability, allowing for broader deployment and improved spatial coverage in air quality assessments.

The system demonstrated consistent performance, with measurement accuracy validated against data from the Andhra Pradesh Pollution Control Board (APPCB). The observed accuracies for ozone, $PM_{2.5}$, temperature, and humidity sensors were ±5.02 μg/m³, ±7.94 μg/m³, ±0.67°C, and ±1.68%, respectively. Seasonal and spatial variations in pollutant levels were evident, with $PM_{2.5}$ concentrations notably higher during the monsoon season and peak traffic hours, highlighting the influence of both meteorological and anthropogenic factors.

While the system exhibited strong performance, certain limitations exist. The sensor accuracy under extreme temperature and humidity conditions was not extensively evaluated, and its long-term stability over several months of deployment is yet to be established. Future improvements may include weatherproofing to support extended outdoor use, integration of solar power for off-grid functionality, and cloud-based storage solutions to enable large-scale data aggregation and analysis. Additionally, the onboard Raspberry Pi presents opportunities to implement lightweight prediction algorithms capable of forecasting meteorological conditions or pollutant concentrations based on historical data. Such features could support early warning systems and enhance decision-making in environmental management. The technology also shows significant potential for citizen science initiatives and urban-scale applications aimed at facilitating real-time, data-driven air quality interventions.

REFERENCES

Abraham, S., Li, X., 2014. A cost-effective wireless sensor network system for indoor air quality monitoring applications. Procedia Comput. Sci. 34, 165–171. https://doi.org/10.1016/j.procs.2014.07.090

Al-Kofahi, M.M., Al-Shorman, M.Y., Al-Kofahi, O.M., 2019. Toward energy efficient microcontrollers and Internet-of-Things systems. Comput. Electr. Eng. 79. https://doi.org/10.1016/j.compeleceng.2019.106457

Baca-López, K., Fresno, C., Espinal-Enríquez, J., Martínez-García, M., Camacho-López, M.A., Flores-Merino, M. V., Hernández-Lemus, E., 2021. Spatio-Temporal Representativeness of Air Quality Monitoring Stations in Mexico City: Implications for Public Health. Front. Public Heal. 8, 1–15. https://doi.org/10.3389/fpubh.2020.536174

Cao, T., Thompson, J.E., 2016. Personal monitoring of ozone exposure: A fully portable device for under $150 USD cost. Sensors Actuators, B Chem. 224, 936–943. https://doi.org/10.1016/j.snb.2015.10.090

Castell, N., National, S., Brito, C. De, Guerreiro, B., 2013. Real-world application of new sensor technologies for air quality monitoring ETC / ACM Technical Paper 2013 / 16. Researchgate.Net 16, 34.

Idrees, Z., Zou, Z., Zheng, L., 2018. Edge computing based IoT architecture for low cost air pollution monitoring systems: A comprehensive system analysis, design considerations & development. Sensors (Switzerland) 18.

https://doi.org/10.3390/s18093021

Jiang, X.Q., Mei, X.D., Feng, D., 2016. Air pollution and chronic airway diseases: What should people know and do? J. Thorac. Dis. 8, E31–E40. https://doi.org/10.3978/j.issn.2072-1439.2015.11.50

Johnson, A.C., 2022. Spatial and Temporal Analysis of Air Pollutants in Jiangsu Province, China. Anthropog. Pollut. 6, 47–54. https://doi.org/10.22034/AP.2022.1943235.1122

Kodali, R.K., Sarjerao, B.S., 2018. MQTT based air quality monitoring. 5th IEEE Reg. 10 Humanit. Technol. Conf. 2017, R10-HTC 2017 2018-Janua, 742–745. https://doi.org/10.1109/R10-HTC.2017.8289064

Kortoçi, P., Motlagh, N.H., Zaidan, M.A., Fung, P.L., Varjonen, S., Rebeiro-Hargrave, A., Niemi, J. V., Nurmi, P., Hussein, T., Petäjä, T., Kulmala, M., Tarkoma, S., 2022. Air pollution exposure monitoring using portable low-cost air quality sensors. Smart Heal. 23. https://doi.org/10.1016/j.smhl.2021.100241

Latif, M.T., Huey, L.S., Juneng, L., 2012. Variations of surface ozone concentration across the Klang Valley, Malaysia. Atmos. Environ. 61, 434–445. https://doi.org/10.1016/j.atmosenv.2012.07.062

Lv, Y., Tian, H., Luo, L., Liu, S., Bai, X., Zhao, H., Lin, S., Zhao, S., Guo, Z., Xiao, Y., Yang, J., 2022. Meteorology-normalized variations of air quality during the COVID-19 lockdown in three Chinese megacities. Atmos. Pollut. Res. 13, 101452. https://doi.org/10.1016/j.apr.2022.101452

Meo, S.A., Abukhalaf, A.A., Alomar, A.A., Alessa, O.M., Sami, W., Klonoff, D.C., 2021. Effect of environmental pollutants PM-2.5, carbon monoxide, and ozone on the incidence and mortality of SARS-COV-2 infection in ten wildfire affected counties in California. Sci. Total Environ. 757, 143948. https://doi.org/10.1016/j.scitotenv.2020.143948

Mohtar, A.A.A., Latif, M.T., Baharudin, N.H., Ahamad, F., Chung, J.X., Othman, M., Juneng, L., 2018. Variation of major air pollutants in different seasonal conditions in an urban environment in Malaysia. Geosci. Lett. 5. https://doi.org/10.1186/s40562-018-0122-y

Motlagh, N.H., Zaidan, M.A., Fung, P.L., Lagerspetz, E., Aula, K., Varjonen, S., Siekkinen, M., Rebeiro-Hargrave, A., Petäjä, T., Matsumi, Y., Kulmala, M., Hussein, T., Nurmi, P., Tarkoma, S., 2021. Transit pollution exposure monitoring using low-cost wearable sensors. Transp. Res. Part D Transp. Environ. 98, 102981. https://doi.org/10.1016/j.trd.2021.102981

Perillo, H.A., Broderick, B.M., Gill, L.W., McNabola, A., Kumar, P., Gallagher, J., 2022. Spatiotemporal representativeness of air pollution monitoring in Dublin, Ireland. Sci. Total Environ. 827, 154299. https://doi.org/10.1016/j.scitotenv.2022.154299

Rathnayake, L.R.S.D., Sakura, G.B., Weerasekara, N.A., Sandaruwan, P.D., 2024. Machine Learning-based Calibration Approach for Low-cost Air Pollution Sensors MQ-7 and MQ-131. Nat. Environ. Pollut. Technol. 23, 401–408. https://doi.org/10.46488/NEPT.2024.v23i01.034

Saminathan, S., Malathy, C., 2024. PM2.5 Concentration Estimation Using Bi-LSTM with Osprey Optimization Method. Nat. Environ. Pollut. Technol. 23, 1631–1638. https://doi.org/10.46488/nept.2024.v23i03.033

Shindler, L., 2021. Development of a low-cost sensing platform for air quality monitoring: application in the city of Rome. Environ. Technol. (United Kingdom) 42, 618–631. https://doi.org/10.1080/09593330.2019.1640290

Vivek, N., Sowjanya, P., Sunny, B., Srikanth, S. V., 2017. Implementation of IEEE 1609 WAVE/DSRC stack in Linux. TENSYMP 2017 - IEEE Int. Symp. Technol. Smart Cities 2–6. https://doi.org/10.1109/TENCONSpring.2017.8070033

Wang, J., Zhao, Y., Xu, M., 2022. Distribution Characteristics of Six Criteria Air Pollutants Under Different Air Quality Levels in Cangzhou City, China. J. Heal. Environ. Res. 8, 9. https://doi.org/10.11648/j.jher.20220801.12